



Highly processable $\text{Mg}_{65}\text{Cu}_{25}\text{Tb}_{10}$ bulk metallic glass

X.K. Xi, D.Q. Zhao, M.X. Pan, W.H. Wang *

Institute of Physics, Chinese Academy of Sciences, Beijing 100080, People's Republic of China

Received 24 March 2004; received in revised form 25 June 2004

Abstract

$\text{Mg}_{65}\text{Cu}_{25}\text{Tb}_{10}$ alloy was cast into glassy rod of 5-mm in diameter in air and argon atmosphere by normal copper mold casting method. The glass-forming ability, ignition and oxygen resistances of the alloy were investigated by X-ray diffraction, differential scanning calorimeter and acoustic measurement. The glass-forming alloy is found to show high ignition and oxygen resistances due to the Tb addition. The beneficial effects of Tb on the glass-forming ability and ignition resistance are discussed.

© 2004 Elsevier B.V. All rights reserved.

PACS: 61.43.Fs; 81.05.Zx; 81.20.-n

Mg-based alloys have great potential as engineering materials for automobile, aircraft and computer industries due to their high specific strength and abundance. However, the Mg alloys applications have been limited because of the low mechanical strength and poor ignition and corrosion resistances. Driven by applications, various Mg alloys have been developed to overcome these shortcomings [1]. Particular alloys are Mg-based bulk metallic glasses (BMGs). It is found that the rod-shaped Mg–Cu(Ni)–Y BMGs with 4–7 mm in diameter prepared by copper mold casting under vacuum or argon conditions have superior specific strength, plasticity and good corrosion resistance [2–7]. Recently, the complex multicomponent Mg–Cu(Zn,Ag)–(Y,Gd)–Pd systems with compressive strength up to 0.8–1.0 GPa were successfully fabricated [8,9]. In this letter, we report that a new highly processable $\text{Mg}_{65}\text{Cu}_{10}\text{Tb}_{10}$ alloy with high glass-forming ability (GFA) and high ignition and oxygen resistances can be readily cast into amorphous rod up to 5 mm in diameter in air atmosphere. The rea-

sons for the improved GFA and ignition and oxygen resistances of the Mg-based BMG are investigated.

Cu–Tb inter-alloy was prepared by arc melting Cu and rare earth (RE) element Tb under a Ti-gettered argon atmosphere in a water-cooled copper crucible. The nominal $\text{Mg}_{65}\text{Cu}_{10}\text{Tb}_{10}$ master alloy was obtained by induction melting the Cu–Tb alloy with Mg in a quartz tube in an Ar atmosphere. The master alloy was then re-melted in air atmosphere and then injected into a copper mold without water cooling to get the rod-shaped sample with 1–5 mm in diameter. For comparison, the master alloy was also re-melted and cast in argon atmosphere. The amorphous nature of the samples was identified by X-ray diffraction (XRD) with CuK_α radiation, and confirmed by differential scanning calorimeter (DSC) performing at a heating rate of 20 K/min. Calorimeter was calibrated for temperature and energy at various heating rates with high purity indium and zinc. The values of the onset temperature for crystallization peak, glass transition and melting were determined from the DSC traces with the accuracy of ± 1 K. The oxygen content of the as-cast cylinders was chemically analyzed by using a carrier gas hot extraction (O/N Analyzer TC-436/Leco) and EDS analysis. The acoustic velocities were measured using a pulse echo overlap method with a measuring

* Corresponding author. Fax: +86 10 8264 0223.

E-mail address: whw@aphy.iphy.ac.cn (W.H. Wang).

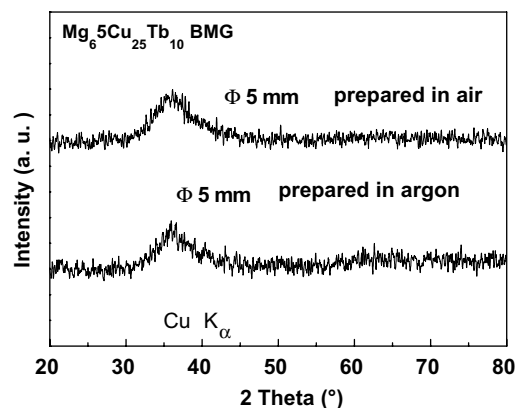


Fig. 1. XRD patterns of $\text{Mg}_{65}\text{Cu}_{25}\text{Tb}_{10}$ alloy prepared in air and argon atmosphere.

sensitivity of 0.5 ns [10]. Elastic constants (e.g., the Yong's modulus E , the shear modulus G , and the bulk modulus K) were derived from the acoustic velocities and the accuracy lies within 0.1% [10].

Fig. 1 shows the XRD patterns of the as-cast rod-shaped $\text{Mg}_{65}\text{Cu}_{25}\text{Tb}_{10}$ alloy (5 mm in diameter) prepared in argon and air atmospheres. Both of the samples exhibit broad diffraction maxima characteristic of glass without obvious crystalline Bragg peaks with the detectable limitation of the XRD. The XRD results indicate the alloy cast both in Ar and air conditions contains mainly amorphous phase. However, in the same preparation condition in our laboratory, a rod-shaped $\text{Mg}-\text{Cu}-\text{Y}$ (the purity of Y is 99.5 at.%) BMG with the similar composition can only be obtained with a maximum diameter of ~ 2 mm. One of the reasons may be the slow quenching rate in our case. These results demonstrate that the GFA and manufacturability of the $\text{Mg}_{65}\text{Cu}_{25}\text{Tb}_{10}$ alloy are much improved with the addition of Tb, and the Mg-based BMG can be melted and cast in air atmosphere without significantly changing its GFA and manufacturability. We even find that Tb-rich Misch rare earth (contain yttrium) can effectively improve the GFA and manufacturability of the $\text{Mg}-\text{Cu}$ alloy as well. The results are summarized in Table 1.

Fig. 2 shows DSC traces of the as-cast $\text{Mg}_{65}\text{Cu}_{25}\text{Tb}_{10}$ alloy prepared in argon and air atmospheres. Both of

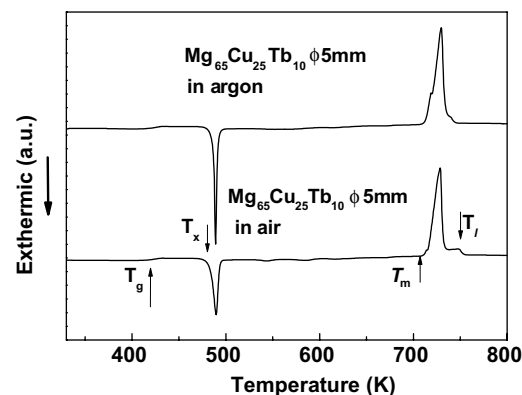


Fig. 2. DSC traces of the $\text{Mg}_{65}\text{Cu}_{25}\text{Tb}_{10}$ alloy prepared in air and argon atmosphere.

the alloys exhibit a distinct glass transition onset at T_g , sharp crystallization onset at T_x and large supercooled liquid region, $\Delta T_x = T_x - T_g$. From the endothermic signal of the melting, one can deduce that the composition of the $\text{Mg}_{65}\text{Cu}_{25}\text{Tb}_{10}$ alloy is very close to the eutectic point. The distinct glass transition, eutectic melting and sharp crystallization events further confirm the amorphous structure of the alloy. The values of T_g , T_x crystallization enthalpy, ΔH_x , melting temperature, T_m and ΔT_x of the alloys prepared under various conditions are listed in Table 1. The reduced glass transition temperature $T_{rg} = T_g/T_m$ [11], which is a critical parameter in determining the GFA of an alloy, is similar for two alloys (see Table 1). The γ [$\gamma = T_x/(T_g + T_l)$], another GFA criterion proposed by Lu and Liu [12], is 0.425 and 0.414 for the alloys prepared in Ar and air conditions, respectively. Comparison of the values of T_{rg} , γ and ΔH_x for the two alloys confirms that the preparation of the alloy in air condition does not markedly deteriorate its high GFA as other BMG-forming alloys do [13–15]. These results indicate that, with the addition of Tb, the GFA of the Mg-based alloy is highly improved and the alloy preparation process is much inert to oxygen environment.

The elastic data obtained from ultrasonic measurements show that there are no significantly difference between the two BMGs prepared in air and Ar atmos-

Table 1

Thermal parameters (heating rate: 20 K/min) of T_g , T_x , ΔT_x , T_m , the liquidus temperature, T_l , T_{rg} , γ and critical diameter, D for the $\text{Mg}_{65}\text{Cu}_{25}\text{Tb}(\text{Y})_{10}$ rods prepared under different conditions

Glass formers	T_g (K)	T_x (K)	ΔT (K)	T_m (K)	T_l (K)	T_{rg}	γ	D (mm)	ΔH_x (J/g)
$\text{Mg}_{65}\text{Cu}_{25}\text{Tb}_{10}$ in argon	414	487	73	723	733	0.573	0.425	5	66
$\text{Mg}_{65}\text{Cu}_{25}\text{Tb}_{10}$ in air	415	483	68	716	753	0.580	0.414	5	65
$\text{Mg}_{65}\text{Cu}_{25}\text{Tb}_9\text{Y}_1$ vacuum	416	489	73	713	732	0.583	0.426	5	66
$\text{Mg}_{65}\text{Cu}_{25}\text{Tb}_8\text{Y}_2$ vacuum	417	492	75	714	734	0.584	0.427	5	67
$\text{Mg}_{65}\text{Cu}_{25}\text{Tb}_7\text{Y}_3$ vacuum	416	488	72	717	736	0.580	0.424	5	66
$\text{Mg}_{65}\text{Cu}_{25}\text{Y}_{10}$ vacuum	414	486	72	734	752	0.564	0.417	2	71

For the thermal parameters of T_g , T_x , ΔT_x , T_m , and T_l , the accuracy is about of ± 1 K. For the crystallization enthalpy, ΔH_x , the accuracy is about of ± 2 J/g.

pheres. For example, the Young's modulus for both of the alloys are about 50 GPa, The density for the two alloys is also almost same ($3.79 \pm 0.01 \text{ g/cm}^3$). From the value of E , the fracture strength for the Mg-BMG is estimated to be in the range of 600–800 MPa [16,17], indicating that the BMG exhibits high fracture strength.

The role of Tb on the GFA of the Mg-alloy can be understood according to the empirical BMG formation criterions [17,18]. Tb has larger radii ($\sim 0.182 \text{ nm}$) comparing with that of Cu and Mg whose radii are 0.128 and 0.160 nm, respectively. The proper Tb addition causes the more optimizing atomic size distributions and increases the complexity of the alloys, which limit the solid-state solubility of these elements. The alloy therefore requires large composition fluctuation to form crystalline phase critical nuclei in supercooled liquid state. Tb also has larger negative heat of mixing with other elements in the alloy, which can form more atomic pairs. Consequently, the packing density and viscous of undercooled liquid are increased and the liquidus temperature is decreased with adequate amount of Tb addition. Thus the stability of supercooled liquid state of the alloy with low atomic diffusivity is enhanced, and then the GFA is improved. On the other hand, the Tb addition sharply decreases the melting temperature of $\text{Mg}_{72}\text{Cu}_{28}$ (the starting alloy of $\text{Mg}_{65}\text{Cu}_{25}\text{Tb}_{10}$) from about 833 K [19] to 723 K. The enthalpy of melting, ΔH_m is related to the entropy of melting, ΔS_m and T_m by the equation: $T_m = \Delta H_m / \Delta S_m$. Therefore, a change in degree of order that increases ΔS_m without affecting ΔH_m causes the decrease of T_m . That is to say, that the Tb addition enhances the GFA of the alloy through inducing a more random closely packed structure of the melt with a lower melting point.

It is intriguing to know the reasons for the high ignition and oxygen resistances of the alloy with Tb addition. During heating in air, we find that the alloy does oxidize (changing color from grey to yellowish red) and a uniform oxide film form and cover the alloy. Near T_m , $\sim 723 \text{ K}$, the alloy deforms significantly because of the sudden volume change at T_m , but the oxide film sustains. Above T_m , the oxide film cracks, but very quickly a new oxide film forms again and prevents the prolonged contact between air and the melt. The oxide film can be maintained well above T_m . No flame burnt up during the melting process. The high ignition resistance of the $\text{Mg}_{65}\text{Cu}_{25}\text{Tb}_{10}$ alloy can be contributed to the oxidation behavior. From the thermodynamic point of view, Tb has a stronger affinity with the oxygen compared with that of Mg and Cu in the alloy. The enthalpy of formation of Tb oxide is in the range of 1800–2000 kJ/mol, and much higher than that of the oxides of other constituent elements (e.g. MgO , 601.6 kJ/mol; CuO , 157.3 kJ/mol) [20]. The reaction between Tb and O is thermodynamically favored compared with other oxidation reactions in the alloy. Therefore, in the melt, Tb element can pro-

hibit the reaction between Mg and oxygen during melting and casting processes. The Mg oxide and Tb oxide acting together makes the alloy oxide film denser than pure Mg or Mg–Cu binary alloy oxide film. Fig. 3 shows the photos of the surfaces of the $\text{Mg}_{72}\text{Cu}_{28}$ (Fig. 3(a)) and the $\text{Mg}_{65}\text{Cu}_{25}\text{Tb}_{10}$ master alloys (Fig. 3(b)). The $\text{Mg}_{65}\text{Cu}_{25}\text{Tb}_{10}$ alloy shows a smooth appearance morphology after melting, indicating its oxide film is quite different from that of the $\text{Mg}_{72}\text{Cu}_{28}$ alloy, which burns up during melting and shows the dark products similar to 'cauliflower' morphology (shown in Fig. 3(b)). The EDS analysis shows that the surface region has much high oxygen content compared to that in the center region. Chemical analysis also show that the composition of the master alloy is close to the nominal composition of $\text{Mg}_{65}\text{Cu}_{25}\text{Tb}_{10}$, and the oxygen content is only about 0.1–0.2 at.%. These results suggest that the oxidation behavior of the Mg-based alloy is changed with the addition of Tb, and the Tb oxide film plays a crucial role in the particularly high ignition and oxygen resistances of this alloy.

In summary, a new Tb-bearing $\text{Mg}_{65}\text{Cu}_{25}\text{Tb}_{10}$ BMG with high GFA (up to 5 mm diameter), high thermal stability, and significant strong ignition and oxygen

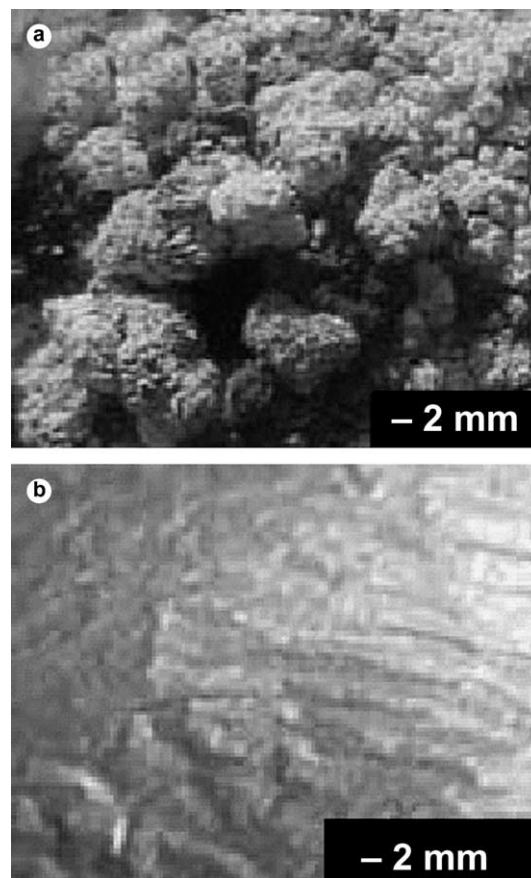


Fig. 3. The photos of master alloy surfaces of the $\text{Mg}_{72}\text{Cu}_{28}$ (a), and the $\text{Mg}_{65}\text{Cu}_{25}\text{Tb}_{10}$ (b).

resistances has been synthesized by a normal casting method in air. The proper Tb addition dramatically enhances the GFA and ignition resistances of the alloy. The RE elements have similar atomic size, chemical and physical properties, we suggest that through the proper addition of other RE elements, other RE-bearing Mg-based BMGs or polycrystalline materials can also be manufactured in air atmosphere too. The results provide an approach to producing new BMGs and improving the manufacturability of the Mg-based BMGs.

Acknowledgment

The authors are grateful for the financial support of the National Natural Science Foundation of China (Grant Nos.: 50371097 and 50321101).

References

- [1] G.L. Song, A. Atrens, *Adv. Eng. Mater.* 5 (2003) 837.
- [2] H. Ma, J. Xu, E. Ma, *Appl. Phys. Lett.* 83 (2003) 2793.
- [3] M.S. Ong, Y. Li, D.J. Blackwood, S.C. Ng, *Mater. Sci. Eng. A* 304 (2001) 510.
- [4] C.H. Kam, Y. Li, S.C. Ng, *J. Mater. Res.* 14 (1999) 1638.
- [5] H.B. Yao, Y. Li, *Surf. Rev. Lett.* 8 (2001) 575.
- [6] A. Kato, T. Zhang, A. Inoue, *Mater. Trans. JIM* 32 (1991) 609.
- [7] A. Inoue, T. Nakamura, *Mater. Trans. JIM* 33 (1992) 937.
- [8] K. Amiya, A. Inoue, *Mater. Trans. JIM* 41 (2000) 1460.
- [9] H. Men, W.T. Kim, D.H. Kim, *Mater. Trans. JIM* 44 (2003) 2141.
- [10] W.H. Wang, R.J. Wang, D.Q. Zhao, *Appl. Phys. Lett.* 74 (1999) 1803.
- [11] D. Turnbull, *Contemp. Phys.* 10 (1969) 473.
- [12] Z.P. Lu, C.T. Liu, *Phys. Rev. Lett.* 91 (2003) 115505.
- [13] X.H. Lin, W.L. Johnson, W.K. Rhim, *Mater. Trans. JIM* 38 (1997) 473.
- [14] W.H. Wang, Z. Bian, D.Q. Zhao, *Intermetallics* 10 (2002) 1249.
- [15] J. Eckert, N. Mattern, M. Seidel, *Mater. Trans. JIM* 39 (1998) 623.
- [16] H.S. Chen, T.T. Wang, *J. Appl. Phys.* 41 (1970) 5338.
- [17] A. Inoue, *Acta Mater.* 48 (2000) 279.
- [18] W.H. Wang, C. Dong, C.H. Shek, *Mater. Sci. Eng. R* 44 (2004) 45.
- [19] Th.B. Massalski, *Binary Alloys Phase Diagrams*, American Society for Metals, Metals Park, OH, 1986.
- [20] O. Kubaschewski, C.B. Alcock, P.J. Spencer, *Material Thermochemistry*, sixth ed., Pergamon Press, 1993.